Electrochemical detection of methanol by platinum/carbon nanotubes nanocomposites synthesised via hydrogen plasma reduction process

Jielin Xu, Shenggao Wang, Zurong Du, Jinlong Zhu, Yi Liu, Wei Zhang, Jianhua Wang

Provincial Key Laboratory of Plasma Chemistry and Advanced Materials, Wuhan Institute of Technology, Wuhan 430073, People's Republic of China
E-mail: tracyxjlin@163.com

Published in Micro & Nano Letters; Received on 16th October 2013; Accepted on 1st November 2013

Platinum (Pt)/carbon nanotube (CNTs) nanocomposites were fabricated on the basis of Pt precursors reduced by hydrogen plasma generated by microwave process. The Pt nanoparticles were uniformly dispersed on multi-walled CNTs. Such nanocomposites exhibit remarkable catalytic performance towards the oxidation of methanol. The concentration of methanol was determined by a chronoamperometric method by using the Pt/CNTs modified glass carbon electrode (Pt/CNTs/GCE) at an oxidation potential of 0.7 V against the saturated calomel electrode. The Pt/CNTs/GCE showed a good performance for detecting methanol because of the unique properties of CNTs which increased the active surface area of the electrode and accelerated the electro transfer. The linear detection range of methanol was determined to be from 2.0×10^{-4} to 10.0 M in two slopes with a detection limit 5×10^{-5} M at a signal-to-noise ratio of 3. The performance of the Pt/CNTs/GCE in terms of stability, linear range and detection limit shows its potential application for methanol detection.

1. Introduction: Direct methanol fuel cells (DMFCs) have attracted much attention because of their advantages of low operating temperature, easy transportation and storage of the fuel, high energy efficiency, low exhaustion and the fast start-up of fuel [1, 2]. DMFCs use methanol as fuel at the anode and oxygen or air as oxidant at the cathode. As the concentration of methanol fluctuates during electrochemical reactions, it affects the cell performance [3, 4]. The concentration of methanol used to increase the power density of cells has been studied [5]. As the concentration of methanol plays a vital role and affects the performance and durability of the fuel cell, it is necessary to develop a robust, reliable and sensitive in situ method to determine the methanol concentration. Several analytical methods have described the determination of methanol among which chromatography [6], surface plasmon resonance (SPR) [7] and Fourier transform infrared spectroscopy [8] are more common. These methods have disadvantages in that they are expensive and far from the on-site where the analysis is actually needed. Recently, numerous studies based on a Pt nanoparticles modified membrane electrode or a glass carbon electrode (GCE) for the determination of methanol concentration were investigated [9–12]. In fact, besides platinum (Pt) nanoparticles, nanocomposites with Pt nanoparticles as one component have also been drawing more and more attention owing to their potential application in many fields [13–15]. Pt nanoparticles are usually supported on multi-walled carbon nanotubes (CNTs), which are of great interest as nanoparticles supports for application in fuel cells because of their large surface area, outstanding electronic transport and structural properties [16–19]. However, to the best of our knowledge, there are limited reports about application in the electrochemical detection of methanol using Pt/CNTs nanocomposites as the modified electrode materials.

In this reported work, Pt/CNTs nanocomposites were synthesised via microwave hydrogen plasma reduction process and we evaluated their application as electrode materials for the electrochemical detection of methanol. It was found that high dispersion Pt nanoparticles were achieved on CNTs and the nanocomposites exhibit remarkable catalytic performance towards the oxidation of methanol. The Pt/CNTs modified glass carbon electrode (Pt/CNTs/GCE) showed a long-term stability, wide linear range and low detection limit.

2. Experimental

2.1. Synthesis and pretreatment of CNTs: Multi-walled CNTs were synthesised with a home-made microwave plasma chemical vapour deposition (MWPCVD) apparatus by using CH_4/H_2 and cobalt as raw materials and catalysts, respectively. The details of the apparatus were given in [20]. During the synthesis of CNTs, the total reaction pressure in the chamber was kept at 4 kPa and the flow rates of CH_4 and H_2 were 3.3 and 55 sccm, respectively. The input power of the microwave plasma was 500 W with a growth time of 1 h.

The CNTs were washed by immersion in concentrated HNO_3 in an ultrasonic bath for 1 h, and then stirred for 5 h at 80°C under magnetic stirring. Later, the wet powder was washed with deionised water until the pH of the filtrated solution was 7. Finally, the powder obtained was dried overnight at 60°C. The purpose of the acid treatment was to implant surface oxides on the surface of the CNTs, creating a number of oxide groups such as carboxylic, carbonyl and hydroxylic groups [21].

2.2. Synthesis of the nanocomposites: The Pt/CNTs nanocomposites were prepared at a CNTs/metal ratio of 80 and 20 wt%, respectively. $H_2PtCl_6{\cdot}6H_2O$ were directly used as the precursors and were dissolved in deionised water. CNTs were poured into the precursor solution. After ultrasonic blending for 2 h, the suspension was heated at 60°C under magnetic stirring to let the solvent evaporate till a smooth thick slurry resulted. The slurry was dried overnight at 60°C in an oven. The obtained agglomerates were ground in an agate mortar. Then, the mixed powder materials (Pt precursors) were put into the MWPCVD chamber, and reduced by hydrogen plasma for 60 min. During the reduction of Pt precursors, the input power of the microwave plasma was 200 W. The total reaction pressure in the chamber was maintained at 3 kPa with an H_2 flow rate of 55 sccm. Finally, the obtained powder materials were cooled to room temperature in N_2 atmosphere.

2.3. Preparation of Pt/CNTs/GCE: Prior to modification, the GCE of 3 mm diameter was polished with an alumina suspension (Φ 0.05 μm) until the surface became mirror-like. 10 mg of Pt/CNTs nanocomposites was dispersed ultrasonically for 30 min in a solution mixture of isopropyl alcohol (2 ml) and 5 wt% Nafion

doi: 10.1049/mnl.2013.0604

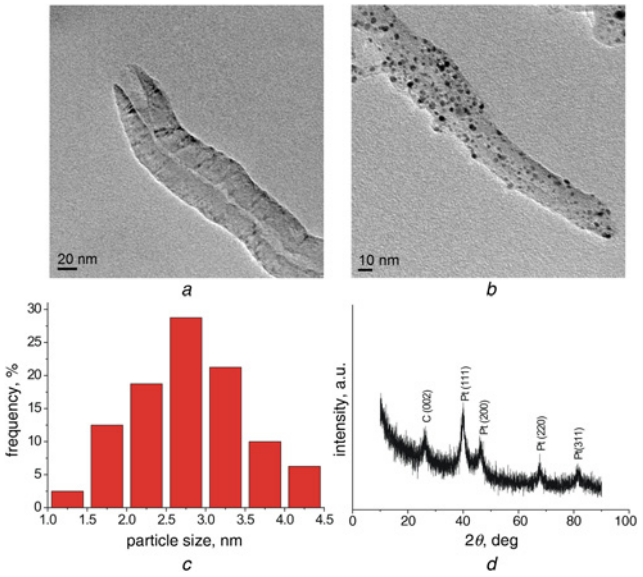

Figure 1 *TEM images, size distribution of supported Pt nanoparticles, and XRD pattern*
a TEM image of CNTs
b TEM image of Pt/CNTs
c Size distribution of supported Pt nanoparticles
d XRD pattern of Pt/CNTs

solution (200 µl) (Dupont, USA). Then, 5 µl of the suspension was coated onto the GCE and dried in an oven at 60°C for 30 min.

2.4. Physicochemical characterisation: Structural characterisation of the Pt/CNTs was carried out by X-ray diffraction (XRD, D2) with Cu Kα radiation at a scanning speed of $0.01° \, s^{-1}$. The crystallite sizes were calculated by means of the Debye-Scherrer equation considering the plan (220) of the face-centred cubic (fcc) structure of Pt. The morphology of Pt/CNTs was investigated using a Model JEM-2100 transmission electron microscope (TEM) operated at 200 kV. The chemical valences of Pt in the prepared Pt/CNTs were analysed by X-ray photoelectron spectroscopy (XPS, VG Multilab 2000).

2.5. Electrochemical measurement: Cyclic voltammetry (CV), linear sweep voltammetry (LSV) and chronoamperometry were executed with a Solartron Modulab ECS analyser. A three-electrode configuration was employed, consisting of a modified GCE (Φ 3 mm) serving as a working electrode, a saturated calomel electrode (SCE) and Pt wire serving as a reference and a

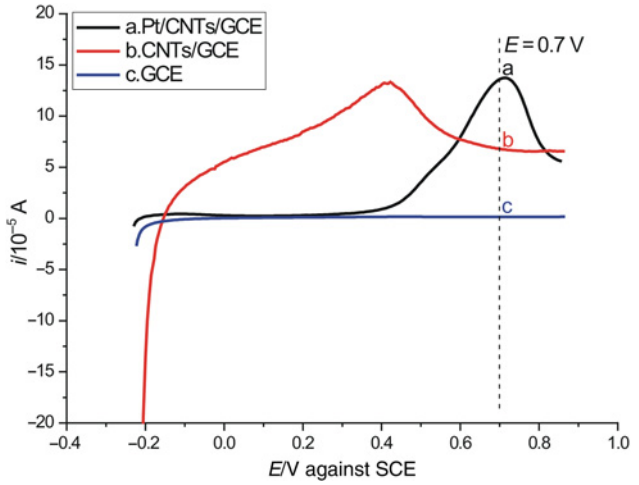

Figure 3 *LSV in 0.1 M H_2SO_4 electrolyte in the presence of 1 M methanol (scan rate: 50 mV s^{-1})*

counter electrode, respectively. All the potentials throughout this Letter are referred to as SCE. All the electrochemical experiments were conducted at room temperature.

3. Results and discussion: The TEM images of the CNTs and Pt/CNTs are shown in Figs. 1*a* and *b*, respectively. The tube-like structure seen in all the TEM micrographs were the multi-walled CNTs and the dark spots represented the Pt nanoparticles, where the wall of the CNTs with some defects was observed (Fig. 1*a*) owing to acid treatment. It can be seen (Fig. 1*b*) that there existed a well-dispersed Pt nanoparticles adlayer on the wall of the CNTs. The particle size distribution histograms of the Pt/CNTs are shown in Fig. 1*c*. The statistical results were obtained from more than 100 Pt nanoparticles and the mean particle size was found to be 2.7 nm. These images clearly reflected that the Pt nanoparticles can be uniformly deposited over surface defect sites of oxidised CNTs by the hydrogen plasma reduction method.

The XRD pattern of the Pt/CNTs is shown in Fig. 1*d*. The peak at $2\theta = 26.2°$ corresponds to the (002) planes of graphitised CNTs and the peaks at $2\theta = 39.9°$, 46.6°, 67.7° and 81.6° can be assigned to the (111), (200), (220) and (311) crystalline planes of the fcc Pt structure. The average crystalline size of Pt supported on CNTs was calculated based on the Pt (220) peak from Scherrer's equation [22] and was found to be 2.6 nm, correlating well with the mean particle size estimated from the TEM image.

The electronic state and surface composition of the Pt/CNTs was also analysed by XPS, as shown in Fig. 2. As the survey scan

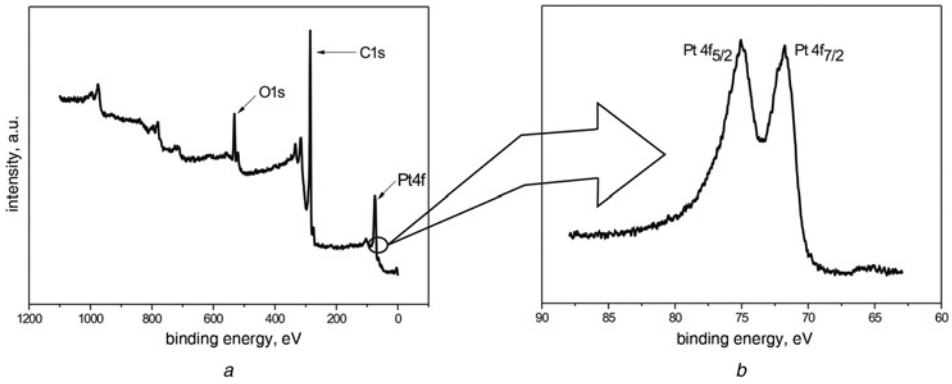

Figure 2 *Survey XPS spectra of Pt/CNTs*
a XPS spectra
b Pt 4f spectra

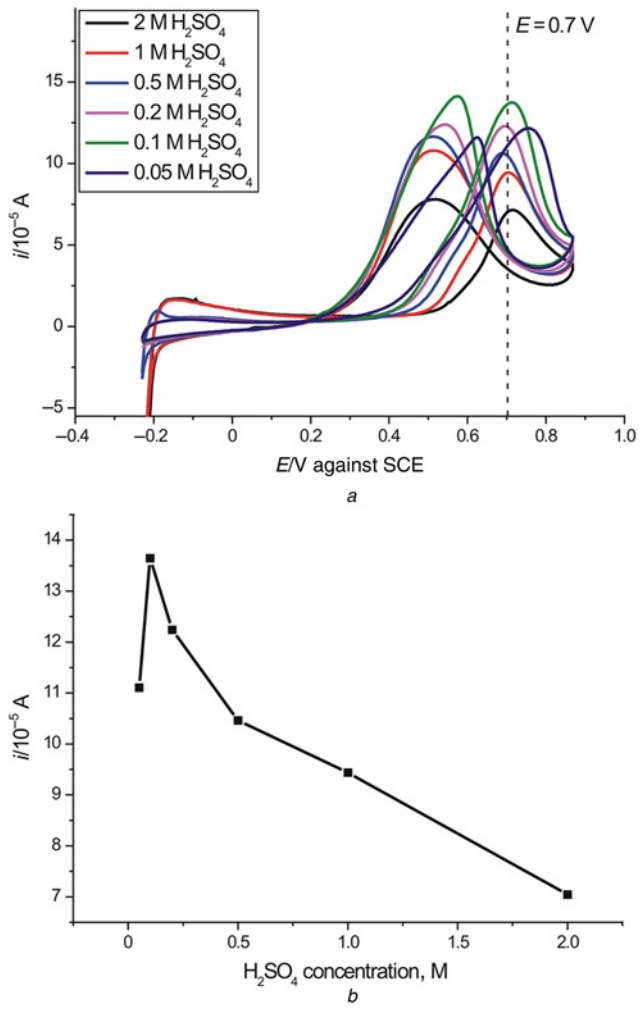

Figure 4 *CVs of Pt/CNTs/GCE*
a CVs in H_2SO_4 electrolyte with different H_2SO_4 concentrations from 0.05 to 2 M in the presence of 1 M methanol (scan rate: 50 mV s^{-1})
b Effect of H_2SO_4 concentration on the peak current value towards 1 M methanol at 0.7 V against SCE

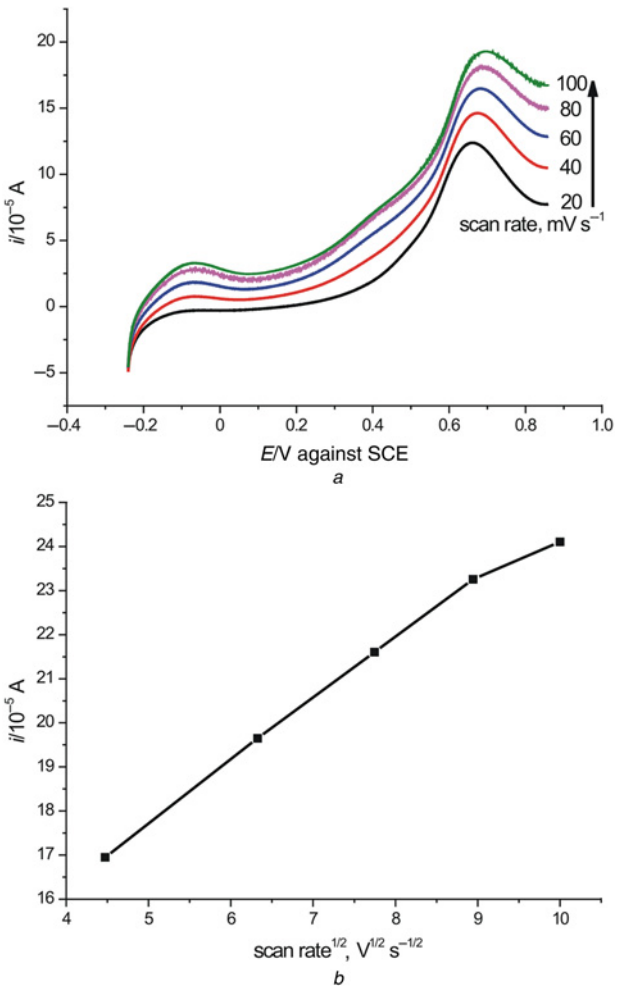

Figure 5 *LSV of Pt/CNTs/GCE*
a LSV in 0.1 M H_2SO_4 electrolyte in the presence of 1 M methanol with different scan rates
b Corresponding plot of current against the square root of scan rate

depicted in Fig. 2*a*, the appearance of the Pt signal demonstrated that the Pt nanoparticles were successfully deposited on the CNTs. Fig. 2*b* represents the XPS signature of the Pt 4f doublet ($4f_{7/2}$ and $4f_{5/2}$) for the Pt nanoparticles supported on the CNTs. The $Pt4f_{7/2}$ and $Pt4f_{5/2}$ peaks appeared at 71.75 and 75.06 eV, respectively, which shifted remarkably to the higher binding energy compared with the standard binding energy of $Pt4f_{7/2}$ and $Pt4f_{5/2}$ for the Pt state (70.83 and 74.23 eV) [23]. The shift of binding energy could be attributed to several factors such as small Pt particle size and defects on the surface of the CNTs, which indicated the strong interaction between the Pt nanoparticles and the CNTs. As Kim and Mitani [24] mentioned previously, the binding energy was shifted towards higher energy with decreasing particle size.

The activity of the bare GCE, CNTs modified GCE (CNTs/GCE) and Pt/CNTs/GCE towards the electrochemical detection of methanol was investigated by linear sweep voltammetry (LSV). Fig. 3 shows the electrocatalytic responses of these electrodes towards the oxidation of methanol in 0.1 M H_2SO_4 electrolyte with the presence of 1 M methanol, both bare GCE (curve c) and CNTs/GCE (curve b) exhibit no response peak at 0.7 V against the SCE corresponding to the oxidation of methanol. It was noteworthy that the CNTs/GCE showed a higher current intensity as compared with the GCE, which could be because of the unique properties of CNTs that increased the active surface area of the electrode and accelerated the electro transfer via improved conductivity and the good affinity of CNTs to methanol. In contrast, the Pt/CNTs/GCE (curve a) displayed a well-defined peak at 0.7 V against the SCE with the highest current intensity, indicating that the role of Pt nanoparticles supported on the CNTs exhibit excellent catalytic performance towards the oxidation of methanol, which was attributed to the charge hopping through the metallic Pt nanoparticles and the effective charge migration through the CNTs.

The effect of the H_2SO_4 concentration on the activity of the Pt/CNTs/GCE was examined. Fig. 4 shows the CVs of the Pt/CNTs/GCE in the H_2SO_4 electrolyte with different H_2SO_4 concentrations from 0.05 to 2 M in the presence of 1 M methanol. It is seen that the current towards the oxidation of methanol at 0.7 V against SCE increased with increasing H_2SO_4 concentration and reached a maximum at a concentration of 0.1 M. Then, the current decreased as the H_2SO_4 concentration was further increased. Therefore the H_2SO_4 concentration of 0.1 M was selected as the supporting electrolyte in the work. Furthermore, the effect of scan rate on the electro-oxidation of methanol on the Pt/CNTs/GCE was also investigated, as shown in Fig. 5. It can be observed that the peak current density was linearly proportional to the square root of the scan rates, which revealed that the electrocatalytic oxidation of methanol on Pt/CNTs/GCE was a diffusion-controlled process [25].

The applicability of the Pt/CNTs/GCE to the detection of methanol was studied. Chronoamperometry experiments at 0.7 V against SCE were conducted in 0.1 M H_2SO_4 electrolyte. Chronoamperograms are shown in Fig. 6*a*, the concentration of methanol varied from 2×10^{-4} to 10.0 M. The current at the end

doi: 10.1049/mnl.2013.0604

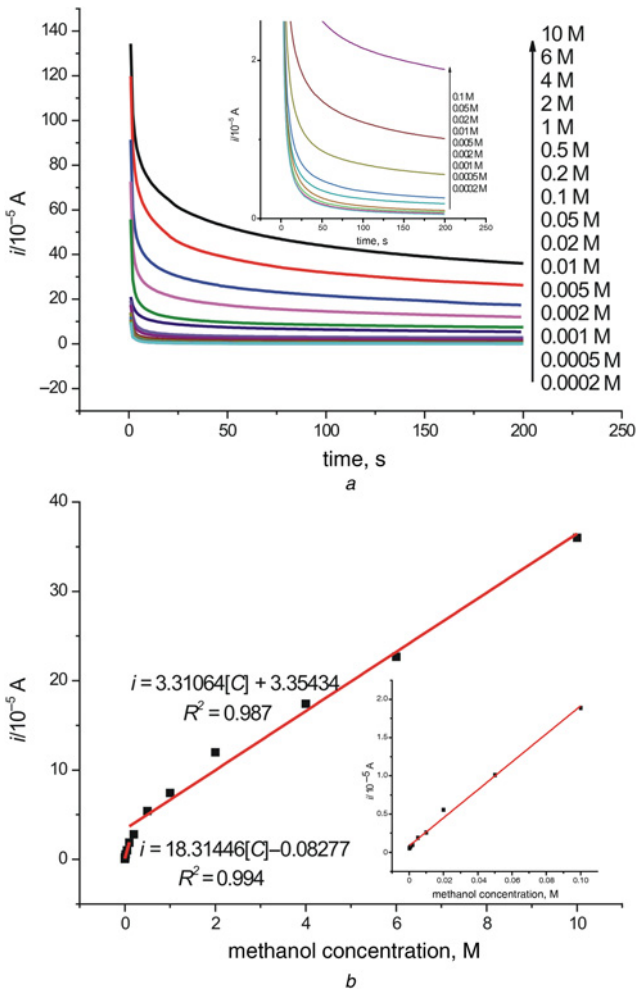

Figure 6 *Chronoamperograms and calibration curve*
a Chronoamperograms observed for the detection of methanol in 0.1 M H_2SO_4 electrolyte at 2×10^{-4} to 10.0 M methanol by using Pt/CNTs/GCE at a potential of 0.7 V against SCE for 200 s
Inset: Local amplification of chronoamperograms for 2×10^{-4} to 0.1 M
b Calibration curve obtained for the detection of methanol on Pt/CNTs/GCE by chronoamperometry
Inset: Calibration plot for 2×10^{-4} to 0.1 M

time of 200 s was recorded and considered to be the response current of the electrode. It can be seen from Fig. 6*b* that the current at the Pt/CNTs/GCE linearly increased with the increase in methanol concentration with a break at 0.1 M. The two dynamic ranges for methanol detection from 2×10^{-4} to 0.1 M and from 0.1 to 10.0 M can be expressed by the two equations: $i = 18.31446\ [C] - 0.08277$ and $i = 3.31064\ [C] + 3.35434$, where $[C]$ is the concentration of methanol as shown in Fig. 6*b*. The

Table 1 Comparison of this work with the literature works regarding the performance of the methanol assays

Type of electrode	Detection limit, M	Linear range, M	Refs
SE/Pt/GC	1×10^{-4}	2.5×10^{-4} – 0.01 and 0.05–10	Park *et al.* [9]
MEA	0.5	0.5–2	Sun *et al.* [11]
MEAs	0.2	0.2–3	Kondoh *et al.* [12]
Pt/CNTs/GCE	5×10^{-5}	2×10^{-4} – 0.1 and 0.1–10	this work

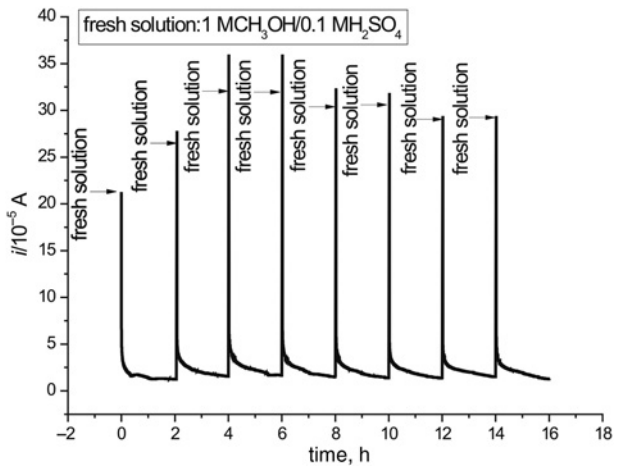

Figure 7 *Stability test (at 0.7 V against SCE) obtained with Pt/CNTs/GCE in 0.1 M H_2SO_4 in the presence of 1 M methanol*

detection limit was estimated to be 5×10^{-5} M (S/N = 3). Compared with most previously reported detection systems [10–12], the Pt/CNTs/GCE described here have a lower detection limit and a wider linear range. The detailed comparison of our present work with others is shown in Table 1.

The stability of the Pt/CNTs/GCE was also evaluated by chronoamperometry at 0.7 V against SCE. A 16 h continuous test was conducted in 0.1 M H_2SO_4 in the presence of 1 M methanol. The solution was refreshed at intervals of 2 h. The result of this test is depicted in Fig. 7. As shown in the Figure, the currents of the Pt/CNTs/GCE maintained a stable current within the operating period, implying the good stability of the Pt/CNTs/GCE.

4. Conclusions: In summary, we have synthesised Pt/CNTs nanocomposites through the hydrogen plasma reduction process. The Pt nanoparticles were uniformly and narrowly dispersed on the CNTs with small particle sizes. The obtained Pt/CNTs have been used for the electrochemical detection of methanol. The Pt/CNTs/GCE showed long-term stability, wide linear range and low detection limit. Compared with the modified electrode in the literature [9], the performance for the detection of methanol was further improved possibly because of the enhanced electron transfer in the Pt–CNTs hybrid system, which was attributed to the charge hopping through the metallic Pt nanoparticles and the effective charge migration through the CNTs. Hence, the Pt/CNTs/GCE is promising for the determination of methanol at the levels expected.

5. Acknowledgments: This work was supported by the National Natural Science Foundation of China (no. 51072140 and 51272187) the Natural Science Foundation of Hubei Province (no. 2013CFA012) and Key Technologies R&D Program of Wuhan (201212211723).

6 References

[1] Chen C.Y., Tsao C.S.: 'Characterization of electrode structures and the related performance of direct methanol fuel cells', *Int. J. Hydrog. Energy*, 2006, **31**, pp. 391–398
[2] Kim D., Cho E.A., Hong S.A., *ET AL.*: 'Recent progress in passive direct methanol fuel cells at KIST', *J. Power Sources*, 2004, **130**, pp. 172–177
[3] Guo H., Nie Z., Ye F., *ET AL.*: 'Technologies for measurement of reactant concentration in direct methanol fuel cells', *Huagong Xuebao*, 2011, **62**, pp. 2413–2420
[4] Cao X., Han J., Yu Z., *ET AL.*: 'Effect of anode and cathode current-collector structure on performance of a passive direct methanol fuel cell', *Adv. Mater. Res.*, 2012, **347**, pp. 3275–3280

[5] Ahmed M., Dincer I.: 'A review on methanol crossover in direct methanol fuel cells: challenges and achievements', *Int. J. Energy Res.*, 2011, **35**, pp. 1213–1228
[6] Wang M.L., Wang J.T., Choong Y.M.: 'A rapid and accurate method for determination of methanol in alcoholic beverage by direct injection capillary gas chromatography', *J. Food Compos. Anal.*, 2004, **17**, pp. 187–196
[7] Manera M.G., Leo G., Curri M.L., *ET AL.*: 'Investigation on alcohol vapours/TiO_2 nanocrystal thin films interaction by SPR technique for sensing application', *Sens. Actuat. B, Chem.*, 2004, **100**, pp. 75–80
[8] Bangalore A.S., Small G.W., Chombs R.J., *ET AL.*: 'Automated detection of methanol vapour by open path Fourier transform infrared spectrometry', *Anal. Chim. Acta*, 1994, **297**, pp. 387–403
[9] Park D.S., Won M.S., Goyal R.N., *ET AL.*: 'The electrochemical sensor for methanol detection using silicon epoxy coated platinum nanoparticles', *Sens. Actuat. B, Chem.*, 2012, **174**, pp. 45–50
[10] Jeng K.T., Huang W.M., Chien C.C., *ET AL.*: 'A versatile electrochemical fuel sensor for direct membrane fuel cell applications', *Sens. Actuat. B, Chem.*, 2007, **125**, pp. 278–283
[11] Sun W., Sun G., Yang W., *ET AL.*: 'A methanol concentration sensor using twin membrane electrode assemblies operated in pulsed mode for DMFC', *J. Power Sources*, 2006, **162**, pp. 1115–1121
[12] Kondoh J., Tabushi S., Matsui Y., *ET AL.*: 'An alternating pulse electrochemical methanol concentration sensor for direct methanol fuel cells', *Sens. Actuat. B, Chem.*, 2010, **147**, pp. 612–617
[13] Roy A.K., Hsieh C.T.: 'Pulse microwave-assisted synthesis of Pt nanoparticles onto carbon nanotubes as electrocatalysts for proton exchange membrane fuel cells', *Electrochim. Acta*, 2013, **87**, pp. 63–72
[14] Ren F.F., Zhou W.Q., Du Y.K., *ET AL.*: 'High efficient electrocatalytic oxidation of formic acid at Pt dispersed on porous poly (o-methoxyaniline)', *Int. J. Hydrog. Energy*, 2011, **36**, pp. 6414–6421
[15] Bonesi A., Asteazaran M., Moreno M.S., *ET AL.*: 'Preparation and evaluation of carbon-supported catalysts for ethanol oxidation', *J. Solid State Electron*, 2013, **17**, pp. 1823–1829
[16] Qian D., Dickey E.C., Andrews R., *ET AL.*: 'Load transfer and deformation mechanisms in carbon nanotube-polystyrene composites', *Appl. Phys. Lett.*, 2000, **76**, pp. 2868–2870
[17] Niu C.M., Sichel E.K., Hoch R., *ET AL.*: 'High power electrochemical capacitors based on carbon nanotube electrodes', *Appl. Phys. Lett.*, 1997, **70**, pp. 1480–1482
[18] De Heer W.A., Châtelain A., Ugarte D.: 'A carbon nanotube field-emission electron source', *Science*, 1995, **270**, pp. 1179–1180
[19] Serp P., Corrias M., Kalck P.: 'Carbon nanotubes and nanofibers in catalysis', *Appl. Catal. A, Gen.*, 2003, **253**, pp. 337–358
[20] Wang S.G., Wang J.H., Ma Z.B., *ET AL.*: 'Vertically aligned carbon nanotubes grown on geometrically different types of surface', *Diam. Relat. Mater.*, 2003, **12**, pp. 2175–2177
[21] Hsieh C.T., Hung W.M., Chen W.Y., *ET AL.*: 'Microwave-assisted polyol synthesis of Pt-Zn electrocatalysts on carbon nanotube electrodes for methanol oxidation', *Int. J. Hydrog. Energy*, 2011, **36**, pp. 2765–2772
[22] Li W.Z., Liang C.H., Zhou W.J., *ET AL.*: 'Preparation and chracterization of multiwalled carbon nanotube-supported platinum for cathode catalysts of direct methanol fuel cells', *J. Phys. Chem. B*, 2003, **107**, pp. 6292–6299
[23] Moudler J.F., Stickle W.F., Sobol P.E., *ET AL.*: 'Handbook of X-ray photoelectro spectroscopy' (PerkinElmer, Eden Prairie, 1992)
[24] Kim Y.T., Mitani T.: 'Surface thiolation of carbon nanotubes as supports: a promising route for the high dispersion of Pt nanoparticles for electrocatalysts', *J. Catal.*, 2006, **238**, pp. 394–401
[25] Bard A.J., Faulkner L.: 'Electrochemical methods: fundamentals and applications' (Wiley, New York, 1980)

doi: 10.1049/mnl.2013.0604